2011 IEEE/RSJ International Conference on
Intelligent Robots and Systems
September 25-30, 2011. San Francisco, CA, USA

Localization Using Ambiguous Bearings from Radio Signal Strength

Jason Derenick, Jonathan Fink and Vijay Kumar

***Abstract*— In this paper, we consider the problem of localizing a mobile robot team capable of measuring ambiguous bearing estimates using received signal strength indicators (RSSI) from radio transceivers (e.g., ZigBee). More precisely, we formulate a robust bearing estimator that leverages anisotropic but symmetric radiation profiles to identify π-periodic bearing estimates between pairs of communicating agents. Utilizing these ambiguous bearing estimates along with compass and odometric measurements, we present a Multi-hypothesis Extended Kalman Filter-based framework that exploits agent motion to resolve the resulting state ambiguity and achieve localization up to translation. Despite the combinatoric nature of our problem, for teams exhibiting certain topological properties, we show that only two initial hypotheses need consideration to recover state. Experimental results from a small team of differential drive robots are presented to demonstrate the utility of our approach. Simulation results are also presented that explore our framework's convergence properties for larger team sizes.**

I. INTRODUCTION

The ability of a robot team to achieve localization is a precondition for most robust control and planning algorithms. Coupling this need with the realization that the control of such systems often requires some level of network communication, it is not surprising that the robotics community has begun exploring the utility of wireless technologies (*e.g.*, WiFi, ZigBee, *etc.*) to facilitate localization in areas where GPS is intermittent or inaccessible. Despite many notable efforts, the problem of effectively exploiting such technology for localization remains an open and active research area.

Towards addressing this challenge, we focus upon robustly localizing a team of mobile robots where agents are equipped with low-power, commodity wireless transceivers for mesh networking. Specifically, we begin by considering a bearing-based approach that, in contrast to previous approaches to RF-based localization, exploits locally generated, anisotropic *radio signal profiles* to estimate ambiguous (π-periodic) bearing estimates between communicating peers. Uniting these estimates with noisy odometric and heading information, we then formulate a Multi-hypothesis EKF-based framework that exploits agent motion to achieve localization.

Our interest in exploring such an approach is motivated by a long-term research objective to develop *minimalistic algorithms* that can be used by robotic platforms featuring reduced hardware and sensing capabilities. As such, for this research, we forgo the use of sensors such as cameras, IMU's, LIDARS, *etc.*, which may not be available to low-cost, sacrificial platforms. Instead, we rely on information from each agent's radio transceiver, a necessity for communication, to facilitate the localization process. Note that we don't attempt to address the hard problem of modeling or learning RF-propagation characteristics which is necessary for traditional RF-based localization methods. Also, while relative bearing measurements would be aided by the use of a directional antenna, this would undermine the primary objective of the radio – efficient and flexible communications.

Jason Derenick, Jonathan Fink and Vijay Kumar are with GRASP Laboratory, University of Pennsylvania, Philadelphia, PA 19104, USA. {jasonder,jfink,kumar}@seas.upenn.edu

The authors gratefully acknowledge support from ARO Grant W911NF-05-1-0219, ONR Grants N00014-07-1-0829 and N00014-08-1-0696, and ARL Grant W911NF-08-2-0004.

II. RELATED WORK

RF–based localization and mapping has been studied extensively in robotics, sensor networks, and communications literature. Recently, [1] considered a Monte–Carlo localization approach where the world is modeled as a WiFi signal strength map in which the robot localizes itself using a continuous perceptual model. [2] also performs an experimental study of RF–based localization using Monte–Carlo methods with additional experimentation to characterize how signal strength varies as a function of environmental variables. [3] considers a probabilistic model that serves to map RSSI values to real–world distance measures. [4] exploits a Gaussian process model to build an *online* signal–strength map that is utilized to provide a maximum likelihood estimate of source location. Additional studies in this area include [5], [6], [7].

Others have explicitly explored bearing–only localization for robot teams and sensor networks. Perhaps most relevant of those is [8] who attempt to explicitly estimate bearing information from RSSI using local motion to enable gradient estimation. Alternatively, radios equipped with angle of arrival (AOA) capability can be used in sensor networks to localize when only some nodes have position information [9]. [10] considers the exploitation of odometric information and relative bearing inferred from cameras to localize teams. Other notable results on this topic include [11], [12], [13].

Bearing-only SLAM also has relevance to this research [14], [15], and [16]. Additionally, others have exploited geometric constraints to facilitate localization [17].

In contrast to this previous research, our approach avoids the use of raw RSSI as a proxy for distance and instead relies on relative bearing-based measurements between communicating peers. As such, we avoid issues of tuning for particular environments and the accompanying accuracy limitations.

III. PROBLEM STATEMENT

Let $\mathcal{R} = \{r_1, \ldots, r_n\}$ denote a set of n uniquely identified mobile robots with time-dependent state vector $x(t) = \left(x_1(t)^T, \ldots, x_n(t)^T\right)^T$ with $x_i(t) \triangleq$

$(x_{i,x}(t), x_{i,y}(t), \theta_i(t))^T \in SE(2)$ denoting the system's state at time t with respect to inertial frame $\mathcal{F}_\mathcal{R}$. This frame is selected by a designated *root* (or *leader*) agent $r_\ell \in \mathcal{R}$, which guides the process. For the sake of convenience, assume that the initial positional state of the root (*i.e.*, $x_{\ell,x,y}(0)$) corresponds to the origin of $\mathcal{F}_\mathcal{R}$.

For applications requiring substantial robot motion with noisy odometry, even non-ambiguous bearing measurements and aligned heading estimates are not sufficient to prevent drift in the team's positional state estimates. As such, the goal of our research is to ultimately recover an estimate of the team's state up to translation with respect to its true state.

Formalizing this objective, we define the following equivalence class of time-dependent states with respect to $x(t)$

$$[x(t)] = \left\{ y(t) \colon \forall i, y_i(t) = x_i(t) + (\tau_{x(t)}, \tau_{y(t)}, 0)^T \right\} \quad (1)$$

and introduce the estimated team state at time t as $\hat{x}(t) = \left(\hat{x}_1(t)^T, \ldots, \hat{x}_n(t)^T\right)^T$ with $\hat{x}_i(t)$ being defined similarly to $x(t)$. Given these definitions, our goal is to formulate a robust framework that converges to and then maintains $\hat{x}(t) \in [x(t)]$ (*i.e.*, $\hat{x}(t) \sim x(t)$) beyond some point in time.

Momentarily deferring discussion of this point until Section V, we turn our attention towards defining the chosen motion and measurement models. Regarding the former, assume each agent caters to the standard velocity model

$$u_i(t) = (v_i(t), \omega_i(t))^T \quad (2)$$

where $v_i(t)$ and $\omega_i(t)$ correspond to translational and rotational velocity inputs at time t with $\hat{v}_i(t) \sim \mathcal{N}(v_i(t), \sigma^2_{v_i})$ and $\hat{w}_i(t) \sim \mathcal{N}(\omega_i(t), \sigma^2_{w_i})$ representing the performed control. We adopt the standard unicycle motion model defined

$$\dot{x}_i(t) = (v_i(t) cos(\theta_i(t)), v_i(t) sin(\theta_i(t)), \omega_i(t))^T. \quad (3)$$

Regarding the measurement model, we assume π-periodic bearing measurements (we justify this assumption in Section IV). Let $\Phi_i = (\phi_{i,1}, \ldots, \phi_{i,i-1}, \phi_{i,i+1}, \ldots, \phi_{i,m})^T$, $\phi_{i,j} \in \mathbb{S}^1$ represent the vector of $(m-1)$ true state-dependent bearings, up to some integer multiple of π, from agent i to each of its m single–hop neighbors, which comprise the set $\mathcal{N}_i \subseteq \mathcal{R} \setminus \{r_i\} \subset \mathcal{R}$. Intuitively speaking, π-periodicity in terms of our bearing estimates means that agent i will attempt to estimate the true bearing to agent j, $\phi_{i,j}$, by receiving an estimate approximating $\phi_{i,j}$ or $\phi_{i,j} + \pi$.

Observe that each estimate can be uniquely represented by adding an offset of 0 or π to the true bearing estimate. As shall be seen, these offsets will be utilized in Section V to define our hypotheses. However, for now, it should be noted that each bearing estimate, although ambiguous, is consistent with its offset (*i.e.*, 0 or π) for all time. Such an assumption is hardly restrictive as shall be seen in Section V.

Let $Z_{\Phi_i} = (z_{\phi_{i,1}}, \ldots, z_{\phi_{i,i-1}}, z_{\phi_{i+1}}, \ldots, z_{\phi_{i,m}})^T$, $z_{\phi_{i,j}} \in \mathbb{S}^1$ represent the vector of π-periodic estimates for agent r_i with respect to its neighbors. We make a standard Gaussian assumption (as evidenced by the results in Section VI) in that $\forall r_i \in \mathcal{R}, \forall r_j \in \mathcal{N}_i, z_{\phi_{i,j}} \sim \phi_{i,j} + \mathcal{N}(0, \sigma^2_{z_{\phi_j}})$. Similarly, let Z_Φ represent the concatenation of these estimates.

Additionally, we assume that agent r_i can estimate its heading in $\mathcal{F}_\mathcal{R}$ (achievable with a compass assuming without loss of generality that $\mathcal{F}_\mathcal{R}$ differs from the global intertial frame $\mathcal{F}_\mathcal{W}$ by a translation), θ_i with $z_{\hat{\theta}_i} \sim \hat{\theta}_i + \mathcal{N}(0, \sigma^2_{z_{\hat{\theta}_i}})$.

Putting all of these pieces together, we now arrive at the following problem statement

Problem 1: Given $\mathcal{R}$ with agents governed by (2) and (3) with initial team-based state $x(0)$ in $\mathcal{F}_\mathcal{R}$, using only the aforementioned noisy odometric measurements, π-periodic bearing estimates, and heading estimates, can a robust framework be developed to yield an estimated state $\hat{x}(t)$ such that $\hat{x}(t) \sim x(t)$ (*i.e.*, the localized state is equivalent to up to translation of the true state) beyond some point in time?

Accordingly, we now begin with the formulation and experimental validation of the proposed bearing estimator.

IV. Bearing Estimation

While antenna design typically strives to be isotropic in its sensitivity, real antennas will inevitably have some orientation dependence. In general a real antenna will have a lobe structure where there exists a bearing along which the antenna is much less sensitive [18].

A generic two-lobe structure can be approximated on a dB scale by

$$\Psi_2(\theta) = 20 \log_{10} \left(\left| \frac{-\cos\left(\frac{1}{2}\pi \cos\theta\right)}{\pi \cos\theta} \right| \right) + 20 \log_{10} \pi + \eta \quad (4)$$

where η is a normalization term to account for the magnitude of the received signal at a particular location. More general lobe structures can be generated by composition of several parameterized versions of (4) where we indicate the number of lobes by the subscript of $\Psi(\theta)$.

Given these antenna profiles, our approach is to gather received signal strength data while rotating the antenna and identify the most likely bearing to the signal source. Let an individual RSSI measurement be $\psi_{i,j}(\theta_k)$ and assume that a relative bearing estimate is computed after sampling $\theta_k \in [0, 2\pi)$. Then, a function

$$\mathcal{E}_\ell(\phi_{i,j}) = \int_0^{2\pi} \left(\psi_{i,j}(\theta_k) - \Psi_\ell(\theta_k - \phi_{i,j})\right)^2 d\theta_k \quad (5)$$

describes the error of the collected measurements given a relative bearing $\phi_{i,j}$. The normalization parameter η is set $\eta = \max_{\theta_k \in [0,2\pi)} \psi_{i,j}(\theta_k)$. Based on empirical evidence, we attempt to fit both one and two-lobe models to the measured data. The best estimate for $\phi_{i,j}$ is then given by the minimum over $\mathcal{E}_1(\phi_{i,j})$ and $\mathcal{E}_2(\phi_{i,j})$,

$$\hat{\phi}_{i,j} = \underset{\phi_{i,j} \in [0,2\pi), \ell \in \{1,2\}}{\operatorname{argmin}} \mathcal{E}_\ell(\phi_{i,j}). \quad (6)$$

The symmetric nature of antenna profiles dictate that this method of bearing measurement will suffer from direction ambiguity, thus driving the focus of this work.

The robots used in these experiments are small indoor ground platforms equipped with a differential drive system, onboard computation, and *802.11a* wireless communication.

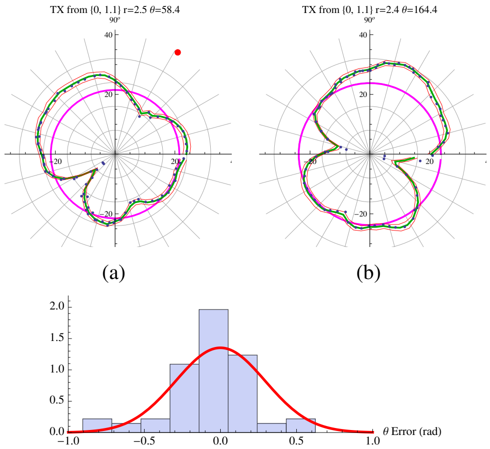

(a) (b) (c)

Fig. 1. Bearing estimator results. Figures 1(a) and 1(b) both depict raw data that enters the bearing estimation process. The magenta circle in each example illustrates $\bar{\psi}_{i,j}$ and the red dot indicates the actual bearing. Figure 1(c) depicts the probability density of estimator error with a histogram over 100 trials to justify our Gaussian approximation.

Each is also outfitted with *Zigbee* radio for mesh-networking. Note that the operational frequency of *802.11a* is 5 GHz and all data logging and experiment monitoring occurred via this alternative frequency to avoid affecting the measurement of RSSI. A *Vicon* motion capture system is used to provide accurate ground truth information for all experiments.

To properly characterize the noise model of our RSSI–based bearing estimator, we conducted over 100 trials where one robot transmitted packets and another rotated in place to compute the bearing measurement in (6). For the purposes of this experiment, we relied on the ground truth data to properly resolve the direction ambiguity in the measurement. Figures. 1(a) and 1(b) show example trials. Figure 1(c) depicts a histogram of the error, demonstrating that it can be approximated by a Gaussian distribution with $\sigma_{z_{\hat{w}_i}} = 17°$.

V. Localization

Our approach is to leverage motion of one or more agents in order to disambiguate the team state via a Multi-Hypothesis Extended Kalman Filter (MH-EKF) and ultimately recover the relative positions of the formation. Our approach in formulating this result is "bottom–up" in the sense that we begin by considering the number of hypotheses necessary to achieve localization using geometric constraints before working our way towards a filter-based solution.

A. Determining the Number of Initial Hypotheses

The utility of any multi-hypothesis framework depends heavily upon the number of initial hypotheses needing consideration. Fortunately, despite its combinatoric nature, our problem is not so ill-conditioned as we can exploit geometric constraints to reduce the feasible set of solutions.

Borrowing terminology from algebraic topology, we abstract the communications network, denoted X, as a chain of 2–simplices, where a 2–simplex is introduced between each triple of communicating agents. Letting $\sigma_{2,ijk}$ denote the 2–simplex introduced by neighboring agent's $r_i, r_j, r_k \in \mathcal{R}$, we define the σ_2–graph of the network topology (see Fig. 2) as the simple, non–reflexive graph $G_{\sigma_2}(X) \triangleq (\mathcal{V}_{\sigma_2}, \mathcal{E}_{\sigma_2})$, where $\mathcal{V}_{\sigma_2} = \{\sigma_{2,ijk} \in X\}$ and the edges are given by the set $\mathcal{E}_{\sigma_2} = \{(\sigma_{2,ijk}, \sigma_{2,stu})\colon \sigma_{2,ijk}, \sigma_{2,stu} \in X, \sigma_{2,ijk} \smile \sigma_{2,stu}\}$, where $\sigma_{2,ijk} \smile \sigma_{2,stu}$ indicates that two distinct 2–simplices share an edge (*i.e.*, they are lower–adjacent).

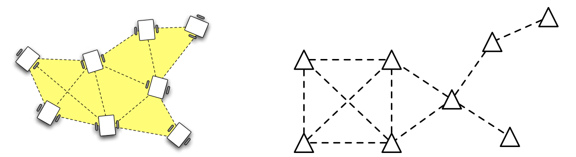

(a) Topology (b) $G_{\sigma_2}(X)$

Fig. 2. (a) A state-dependent network topology, X, decomposed into 2-simplices. (b) $G_{\sigma_2}(X)$. Assuming each agent is involved in at least a single 2-simplex in X, A connected $\sigma_2 - graph$ is a sufficient condition for localization with π-periodic bearings and only 2-initial hypotheses.

Given this construct, we can now establish the number of initially feasible hypotheses. However, it should be noted that our approach to the localization process is to represent hypotheses, corresponding to a set of feasible states, as angular offsets of 0 or π with respect to each bearing measurement in the system. As such, in generating an initially feasible set, it is sufficient to establish that each such hypothesis at time $t = 0$ provides a scale-free representation of the system. Recovering the system scale will be the iterative result of node motion with odometric measurements.

Theorem 5.1: Let $\mathcal{R}$ represent a team of $n \geq 3$ robots with root r_ℓ. Assume $G_{\sigma_2}(X)$ is connected with each agent involved in at least a single 2-simplex. Assume all heading and π-periodic bearing measurements are perfect. The number of initial hypotheses required to achieve localization up to translation and scale with respect to $\mathcal{F}_\mathcal{R}$ is 2.

Proof: By construction. Without loss of generality, assume the initial state of the root r_ℓ (*i.e.*, x_ℓ) is given by $(0, 0, \theta_\ell)^T$. Let $r_j \in \mathcal{N}_\ell$ denote some neighbor of r_ℓ chosen randomly. r_j is denoted the *seed agent*. Although each agent's bearings are ambiguous, we can still exploit knowledge of heading (in fact, this constraint can be theoretically relaxed to allow for systems where heading is also π-periodic in $\mathcal{F}_\mathcal{R}$.) to determine position. To see this, observe that node r_ℓ has two possible choices of bearing to agent r_j, $\phi_{l,j}$ or $\phi_{l,j} + \pi$. Without loss of generality, assume r_ℓ chooses the bearing $\phi_{l,j}$. Given $\phi_{l,j}$, localize the position of r_j, up to scale with respect to r_ℓ, by setting x_j = $(cos(\phi_{l,j} + \theta_\ell), sin(\phi_{l,j} + \theta_\ell), \theta_j)^T$.

Given x_ℓ and x_j, observe that by the connectivity of $G_{\sigma_2}(X)$, $\exists\ r_k \in \mathcal{R}, \sigma_{2,ljk} \in X$. To obtain the position of r_k, begin by considering the line $y_{\ell,k} \in \mathcal{F}_\mathcal{R}$ passing through $(x_{\ell,x}, x_{\ell,y})^T$ with normal $(-sin(\phi_{l,k} + \theta_\ell), cos(\phi_{l,k} + \theta_\ell))^T$ Similarly, consider the second line, $y_{j,k} \in \mathcal{F}_\mathcal{R}$, passing through $(x_{j,x}, x_{j,y})^T$ with normal $(-sin(\phi_{j,k} + \theta_j), cos(\phi_{j,k} + \theta_j))^T$. Employing a straightforward triangulation, we see that the correct, scale–consistent, relative position for r_k (*i.e.*,$(x_{k,x}, x_{k,y})^T$) is $y_{\ell,k} \cap y_{j,k}$.

After localizing r_k, the connectivity of G_{σ_2} dictates that (i) there exists a pair of localized agents with an unlocalized common neighbor or (ii) all agents have been assigned a positions that is consistent up to scale. In (i), continue construction by choosing two localized agents having such a neighbor and utilize their positions and π-periodic bearing estimates to generate the lines for triangulating the position of the common node (see Fig. 3). Reiterate this process until all agents have been localized.

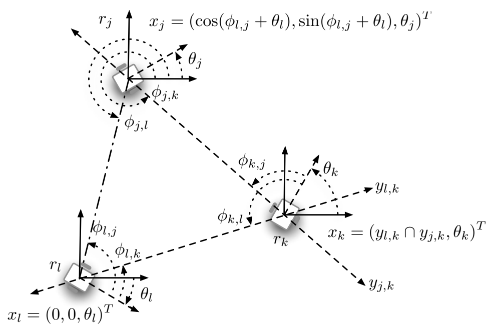

Fig. 3. Assuming r_ℓ has an initial state $(0, 0, \theta_\ell)^T$ and π-periodic bearing estimates to $r_j \in \mathcal{N}_\ell$, r_ℓ can seed the generation of a scale-free hypothetical state for the formation by simply assigning r_j the state $(cos(\phi_{l,j}+\theta_\ell), sin(\phi_{l,j}+\theta_\ell), \theta_j)^T$. Given x_i and x_j, their headings, and π-periodic bearings of each to common neighbor r_k, the pair can recover a scale-consistent positional state by triangulation.

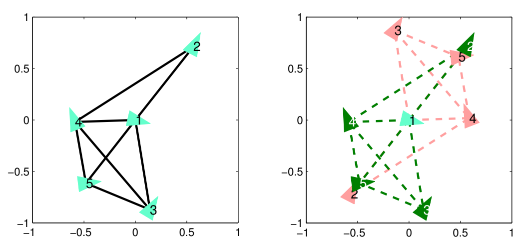

(a) Robot Formation (b) Both Generators

Fig. 4. (a) Five stationary robots in a mesh topology. (b) Generators for each of the two equivalence classes representing scale-free, initial positional configurations r_ℓ corresponds to agent 1 (origin) in the configuration.

The result of this construction is a scaled, feasible representation of the original team formation shape that may be mirrored in position (but not heading, since that value is known to the agent) about the origin with respect to the true state. It represents a single positional hypothesis.

To obtain a second scaled representation of the team formation, start the construction anew; however, this time, choose $\phi_{l,j} + \pi$ as the bearing from r_ℓ to the seeding agent r_j. Figure 4 illustrates this idea.

Finally, it is straightforward to see that if r_ℓ chooses any seed agent other than r_j, the same two configurations will emerge, just at a different scale. This is the case because the headings and π-periodic bearing values across the team remain the same in spite of the choice of seed agent. ■

A key implication of Theorem 5.1 is that the up–to–scale positional ambiguity of the team hinges upon the ability of r_ℓ to resolve its ambiguity in bearings. This is a key point, because it implies, in theory, that the motion of only a single leader node is required to resolve positional localization of the team up to some scale factor.

B. Generating Reference Bearings

In the proof of Theorem 5.1, we describe a method for finding a consistent set of relative bearings across the team. We denote these as the reference bearings $\tilde{\Phi}$. Finding $\tilde{\Phi}$ in the presence of noisy measurements complicates matters and we propose an iterative, distributed process that exploits local scale-free estimates of neighbors' *coarse* positions to compute a consistent set of feasible bearings. Due to the importance of reference bearing initialization, we assume each node computes a robust bearing estimate based on repeated measurements and low-level filtering (*e.g.*, RANSAC [19]).

Algorithm 1 genInitReferenceBearings($X, \hat{\Phi}$)

Require: $G_\sigma(X)$ is connected.
Σ_2 = getAll2SimplicesInTopology(X)
$\sigma_{2,ijk}$ ←get2SimplexWithAgent(r_ℓ,Σ_2)
loop
  $\hat{x}_{ijk}, \hat{\phi}_{\ell jk}$ ← doCoarseScaleFreeLoc($\sigma_{2,ijk}$)
  $\hat{b}_{ijk}$ ← getBearingsFromLocState($\hat{x}_{ijk}$)
  $\hat{\phi}_{ijk}$ ← getBearingsConsistentWithState($\hat{\phi}_{ijk}, \hat{b}_{ijk}$)
  if numProcessed(Σ_2) > 1 **then**
    $\hat{\phi}_{ijk}$ ← makeConsistentWithPrev($\hat{\phi}_{ijk}, \sigma_{prev}$)
  end if
  Σ_2 ← assocBearingsWith2Simplex($\sigma_{2,ijk}$,$\hat{\phi}_{ijk}$)
  Σ_2 ← mark2SimplexAsProcessed($\sigma_{2,ijk}$)
  if allProcessed(Σ_2) **then**
    $\hat{\Phi}$ ← mapSigma2ToAgentBearingVector(Σ_2)
    return $\hat{\Phi}$
  end if
  $\sigma_{2,ijk}$ ← getLowerAdjacent2Simplex($\Sigma_2, \sigma_{2,ijk}$)
end loop

Algorithm 2 doCoarseScaleFreeLoc($\sigma_{2,ijk}$)

$\hat{x}_i \leftarrow (0, 0, \hat{\theta}_\ell)^T$
$\hat{\phi}_{i,j}$ ← getPiPeriodicBearingFromTo(r_i,r_j)
$\hat{\phi}_{i,k}$ ← getPiPeriodicBearingFromTo(r_i,r_k)
$\hat{\phi}_{j,k}$ ← getPiPeriodicBearingFromTo(r_j,r_k)
$\hat{x}_j \leftarrow (cos(\hat{\phi}_{l,j} + \hat{\theta}_i), sin(\hat{\phi}_{l,j} + \hat{\theta}_i), \hat{\theta}_j)^T$
$\hat{y}_{i,k}$ ← getLine($\hat{x}_i, \hat{\phi}_{i,k}$)
$\hat{y}_{j,k}$ ← getLine($\hat{x}_j, \hat{\phi}_{j,k}$)
$\hat{x}_k \leftarrow \hat{y}_{i,k} \cap \hat{y}_{j,k}$
return $(\hat{x}_i, \hat{x}_j, \hat{x}_k)^T$, $(\hat{\phi}_{i,j}, \hat{\phi}_{i,k}, \hat{\phi}_{j,k})^T$

Algorithm 1 operates by iterating over each 2-simplex in our topology, X. At its core is a scale-free, coarse localization (see Alg. 2) that triangulates a common neighbor by two localized nodes to yield a coarse state estimate. The key to this approach is the realization that such an estimate is often accurate enough to recover consistent bearings for the triple of agents.

It begins be decomposing the network topology into 2-simplices and seeds the process by choosing a 2-simplex associated with the selected root, r_ℓ (Lines 1-2). It then invokes (Line 4) the aforementioned coarse, scale-free localization to recover a relative, positional state estimate for the triple of agents involved in the 2-simplex. Given this result, it computes bearings based on each node's heading and scale-free position estimate. Although not perfect, these bearings can be utilized to choose bearings within the triple of agents that are most consistent with the given state (Lines 5-6). Note that the algorithm could also exploit a RANSAC style voting scheme among the three agents at this step.

After considering the first 2-simplex, the initial set of bearings are associated and the simplex is marked as processed (Lines 10-11). Next, it chooses another 2-simplex in the topology that is lower-adjacent to one of the other 2-simplices already processed (Line 16) and the loop reiterates. Upon execution of the subsequent iterations, an additional step is performed (Line 8) to ensure the bearings of the new simplex are consistent with the bearings of the lower-adjacent predecessors in Σ_2.

C. A Multi-hypothesis EKF-based Framework

Taking (2) as the process model, the full state $x(t)$, and the measurement model outlined in Section III, our objective is to maximize the mixture of Gaussians, $bel(x(t))$, given by

$$\frac{1}{\sum\limits_{\forall h} \gamma_h(t)} \sum_{\forall h} \gamma_h(t) \frac{e^{-\frac{1}{2}(x(t)-\mu_h(t))^T \Sigma_h(t)(x(t)-\mu_h(t))}}{det(2\pi\Sigma_h(t))} \tag{7}$$

where the hypotheses are indexed by $h \in \left\{\tilde{\Phi}, \tilde{\Phi}+\pi\right\}$ and $\gamma_h(t)$ represents the likelihood of the current hypothesis with respect to measurement history. More rigorously, $\gamma_h(t)$ is the measurement likelihood function

$$L(Z_{\Phi,h}(t)|x_h(t)) = \Pi_{i=0}^{t} P(x_h(t-i)|Z_{\Phi,h}(t-i)) \tag{8}$$

As mentioned in the previous section, motion shall be exploited to resolve state ambiguity and ultimately recover the formation scale; however, in order for our filter to converge, $\tilde{\Phi}$ will need to be tracked over time. Fortunately, this is easily done by enforcing the constraint that motion between measurement updates is small and exploiting knowledge of the reference bearings from the previous measurement round.

VI. Results

A. Experimental

A three robot experiment was conducted as depicted in Figs. 6(a)-6(c) where two agents are stationary while a third agent, r_ℓ, moves through an elliptical trajectory. The experimental hardware corresponds to that of Section IV. In this particular experiment, the following parameters were chosen based on testbed analysis: $\sigma_{z_{\phi_i}} = 15°$, $\sigma_{z_{\theta_i}} = 10°$, $\sigma_{v_i} = 0.05m/s$, and $\sigma_{w_i} = 10°/s$. Since our platform does not include a magnetometer, we emulate this noisy sensor using heading measurements from a motion capture system.

In this trial, all robots belong to the same neighborhood so that relative bearing measurements are made between all pairs of robots resulting in fast convergence of team-state depicted in Fig. 5. Observe that after only 7 measurement

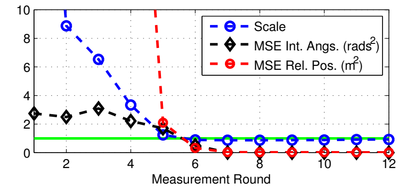

Fig. 5. The scale, MSE of formation interior-angles, and relative position with respect to r_ℓ in the experimental trial depicted in Fig. 6.

rounds, the team obtains a formation that is nearly consistent with scale of ≈ 0.87 (shown converging to 1) and has an MSE over the interior angles (used to capture scale-independent formation) and relative position of $\approx 0.45 degs^2$ and $\approx 0.027m^2$. After completing 12 measurement rounds, the scale is ≈ 0.92 with MSE values being $\approx 0.05 degs^2$ and $\approx 0.033m^2$.

B. Simulations

In order to analyze the performance of our algorithms on larger scale systems, we turn to a simulation infrastructure where relative bearing measurements, odometry, and compass headings are all affected by appropriate noise models to match our experimental system as closely as possible. In this simulation environment, we consider a larger 15 robot system in a mesh-like topology as depicted in Fig. 7(a).

When a single root node is mobile, as in our experimental trial, convergence of the state estimate is quite poor as depicted in Fig. 7(b) where even after 100 measurement rounds, the localization accuracy is on the order of 5m^2 (compared to 0.033m^2 obtained after 7 rounds in the three robot experiment). It is clear that this convergence rate is related to the topology of the network and how nodes are connected to the mobile root node. The results in Fig. 7(b) demonstrate that as more nodes exhibit motion, the convergence rate improves and the filter is able to achieve similar accuracy as in the three robot experiment.

If we examine a scale-free metric (in this case, the MSE over interior angles of 2-simplices within the formation) for the performance of the filter on large systems, convergence occurs noticeably faster as depicted in Fig. 7(c). Despite the slow convergence of scale in the single mobile root case, after only 15 measurement rounds the MSE over the system's 51 interior angles less than $0.02 rads^2$, while the MSE in relative positional error is $5.85m^2$. In other words, the positional error is due the difference in formation scales and we are able to quickly recover a scale-free localization.

VII. Conclusion

The problem of localizing a team of mobile robots using π-periodic bearing estimates was considered. Motivating this research was the formulation of a robust, RF-based bearing estimator that exploits locally generated signal strength profiles between communicating neighbors to estimate π-periodic bearings. To resolve the resulting ambiguities in state, we formulate a MH-EKF-based framework for localizing the team (up to translation) that exploits agent motion to

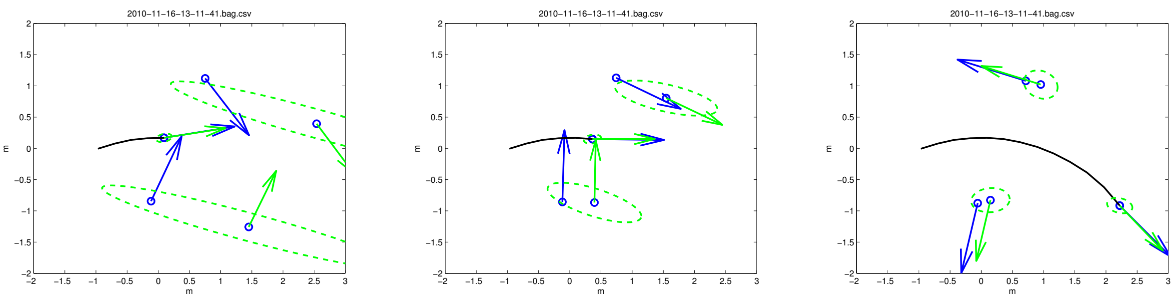

(a) 5 Rounds (b) 6 Rounds (c) 12 Rounds

Fig. 6. Snapshots of the three robot experiment demonstrating the convergence of the proposed filter with relative bearing estimates based on RSSI measurements from off-the-shelf *Zigbee* radios. The state estimate is provided relative to the root node which starts at $(-1, 0)$ m. Ground truth is depicted by blue arrows while the EKF estimate is indicated with green arrows and confidence ellipsoids.

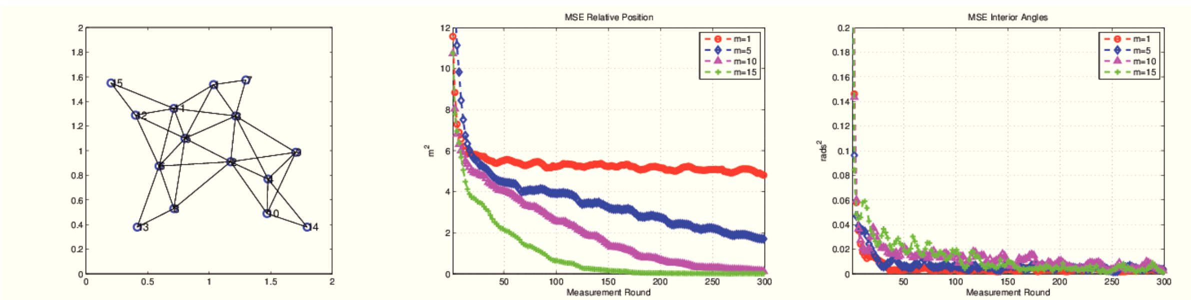

(a) (b) (c)

Fig. 7. (a) Initial positional configuration of 15 robot simulation. Lines between robots indicate communication connectivity and the ability to make relative, π-periodic bearing measurements. (b) Convergence of the mean-squared-error of the filter. m denotes the number of mobile nodes. (c) Performance of scale-free localization for the team. The metric for scale-free localization is computed over the error in interior angles over each 2-simplex in the graph.

resolve ambiguities and recover scale. Despite the combinatoric nature of the problem, our analysis reveals that under certain topological conditions, only 2 initial hypotheses need consideration! We also present both experimental and simulation results demonstrating the utility of the framework.

REFERENCES

[1] J. Biswas and M. Veloso, "WiFi Localization and Navigation for Autonomous Indoor Mobile Robots," in *IEEE International Conference on Robotics and Automation, 2010. ICRA '10*, May 2010.

[2] A. Howard, S. Siddiqi, and G. S. Sukhatme, "An Experimental Study of Localization Using Wireless Ethernet," in *Springer Tracts in Advanced Robotics: Field and Service Robotics*, vol. 24, 2006, pp. 145–153.

[3] S. Zickler and M. Veloso, "RSS-Based Relative Localization and Tethering for Moving Robots in Unknown Environments," in *IEEE International Conference on Robotics and Automation, 2010. ICRA '10*, May 2010.

[4] J. Fink and V. Kumar, "Online Methods for Radio Signal Mapping with Mobile Robots," in *IEEE International Conference on Robotics and Automation, 2010. ICRA '10*, May 2010.

[5] B. Ferris, D. Fox, and N. Lawrence, "Wifi-slam using gaussian process latent variable models," in *Proc. of the 20th Int. Joint Conf. on Artificial Intelligence, 2007. IJCAI'07*, 2007, pp. 2480–2485.

[6] A. Awad, T. Frunzke, and F. Dressler, "Adaptive Distance Estimation and Localization in WSN using RSSI Measures," in *In 10th EUROMICRO Conference on Digital System Design - Architectures, Methods and Tools (DSD 2007)*. IEEE, 2007, pp. 471–478.

[7] J. Graefenstein, A. Albert, P. Biber, and A. Schilling, "Wireless node localization based on RSSI using a rotating antenna on a mobile robot," in *6th Workshop on Positioning, Navigation and Communication (WPNC 2009)*, Mar 2009, pp. 253 – 259.

[8] K. Dantu, P. Goyal, and G. Sukhatme, "Relative Bearing Estimation from Commodity Radios," in *ICRA'09: Proceedings of the 2009 IEEE international conference on Robotics and Automation*. Piscataway, NJ, USA: IEEE Press, 2009, pp. 3215–3221.

[9] D. Niculescu and B. Nath, "Ad hoc positioning system (APS) using AOA," in *IEEE Societies INFOCOM 2003. 22nd Annual Joint Conf. of the IEEE Comp. and Comm.*, 2003, pp. 1734–1743.

[10] M. Deans, "Bearings-only localization and mapping," Ph.D. dissertation, Robotics Institute, Carnegie Mellon University, Pittsburgh, PA, September 2005.

[11] B. Shirmohammadi and C. J. Taylor, "Distributed Target Tracking Using Self Localizing Smart Camera Network," in *Proceedings of the International Conference on Distributed Smart Cameras (ICDSC'10)*, Atlanta, GA, August 2010.

[12] G. Piova, I. Shames, B. Fidan, F. Bullo, and B. Anderson, "On frame and orientation localization for relative sensing networks," in *47th IEEE Conference on Decision and Control, CDC 2008.*, December 2008, pp. 2326 –2331.

[13] K. Briechle and U. Hanebeck, "Localization of a mobile robot using relative bearing measurements," *Robotics and Automation, IEEE Transactions on*, vol. 20, no. 1, pp. 36 – 44, feb. 2004.

[14] F. Dellaert, F. Alegre, and E. Martinson, "Intrinsic Localization and Mapping with 2 applications: Diffusion Mapping and Macro Polo localization," in *IEEE International Conference on Robotics and Automation (ICRA '03)*, vol. 2, sep 2003, pp. 2344 – 2349.

[15] N. Trawny and S. I. Roumeliotis, "A Unified Framework for Nearby and Distant Landmarks in Bearing-Only SLAM," in *Proceedings of the IEEE International Conference on Robotics and Automation (ICRA)*, vol. 1, Orlando, FL, May 15 – May 19 2006, pp. 1923–1929.

[16] T. Lemaire, C. Berger, I.-K. Jung, and S. Lacroix, "Vision-Based SLAM: Stereo and Monocular Approaches," *International Journal of Computer Vision*, vol. 74, pp. 343–364, September 2007.

[17] M. S. K.O. Arras, J.A. Castellanos and R. Siegwart, ""feature-basedmulti-hypothesis localization and tracking using geometric constraints"," *Robotics and Autonomous Systems (Elsevier)*, vol. Vol. 44, pp. pp.41–53, 2003.

[18] C. A. Balanis, *Antenna Theory: Analysis and Design*. Wiley-Interscience, 2005.

[19] M. A. Fischler and R. C. Bolles, "Random sample consensus: a paradigm for model fitting with applications to image analysis and automated cartography," *Commun. ACM*, vol. 24, no. 6, pp. 381–395, Jun 1981.